Surface modification of $MgAl_2O_4$ (111) for growth of high-quality ZnO epitaxial films

Z. Q. Zeng, Y. Z. Liu, H. T. Yuan, Z. X. Mei, and X. L. Du[a)]
Beijing National Laboratory for Condensed Matter Physics, Institute of Physics, Chinese Academy of Sciences, Beijing 100080, China

J. F. Jia and Q. K. Xue[b)]
Department of Physics, Tsinghua University, Beijing 100084, China

Z. Zhang
Beijing University of Technology, Beijing 100022, China

(Received 31 August 2006; accepted 22 January 2007; published online 22 February 2007)

A magnesium wetting layer was used to modify the surface structure of $MgAl_2O_4$ (111) substrate to achieve growth of high-quality ZnO film by radio frequency plasma-assisted molecular beam epitaxy. It is found that this magnesium layer plays a crucial role in 30° rotation domain elimination, defect density reduction, and polarity control of ZnO film, as demonstrated by *in situ* reflection high-energy electron diffraction and *ex situ* transmission electron microscopy. Atomic force microscopy observation shows smooth ZnO surfaces with clearly resolved atomic steps of the films. © *2007 American Institute of Physics*. [DOI: 10.1063/1.2679171]

ZnO is a direct band gap oxide semiconductor of wurtzite structure. Its most unique property is the large exciton binding energy of 60 meV, a very important parameter for low-threshold excitonic laser diodes (LDs).[1] Although bulk ZnO substrate is commercially available,[2] high-quality ZnO epitaxial films achieved so far were grown on heterogeneous substrates[3] among which sapphire (0001) was commonly used due to its high crystal quality and low cost. However, similar to the case of GaN epitaxy on sapphire (0001), well-known 30° in-plane rotation defect appears in the ZnO epitaxial films, which makes it very difficult to obtain high-quality cavity mirrors of ZnO LDs by cleaving the sapphire substrate.[4] High-quality GaN LD cavities could be obtained on $MgAl_2O_4$ (111) substrate simply by cleavage along the $[\bar{1}10]$ direction,[4] indicating that $MgAl_2O_4$ (111) can be a promising substrate for fabrication of ZnO LD cavity due to the similarities between ZnO and GaN.

$MgAl_2O_4$ belongs to the cubic crystal system ($Fd3m$) and has a spinel crystal structure. Along the [111] direction, the stacking sequence of atoms is –O–Al–O–Mg–Al–Mg–O– and O atoms form a face-centered-cubic sublattice with Al and Mg atoms occupying half of the octahedral and oneeighth of tetrahedral sites, respectively. According to the model by Fang *et al.*, the most stable (111) surface is terminated by oxygen atoms.[5] Chen *et al.* attempted to grow ZnO on this surface by oxygen plasma exposure.[6] Our experiments show that when ZnO was directly grown on the above-mentioned surface, in many cases 30° rotation domains were formed due to the distortion of oxygen sublattice. Control of the substrate surface structure is critical for reduction of rotation domains and inversion domains.[7,8] In this work, by using Mg modification of O-terminated $MgAl_2O_4$ (111) surface, we eliminated the 30° rotation domains and inversion domains and obtained high-quality ZnO films.

A radio frequency (rf) plasma-assisted molecular beam epitaxy (MBE) system (OmniVac) (Refs. 9 and 10) was used to grow ZnO films on $MgAl_2O_4$ (111) substrates. The substrates were degreased in trichloroethylene and acetone and rinsed with de-ionized water before introducing them into the load lock. In the growth chamber, they were thermally cleaned at 780 °C for 20 min and then pretreated by oxygen radicals for 30 min with a rf power of 400 W and an oxygen flux of 2.0 SCCM (SCCM denotes cubic centimeters per minute at STP) at a low substrate temperature of 260 or 130 °C. For sample A, a conventional two-step growth, i.e., a low temperature buffer layer growth at 260 °C and a high temperature growth at 650 °C, was directly performed after oxygen radical pretreatment at 260 °C. Formation of 30° rotation domains in ZnO buffer was observed. For sample B, Mg was deposited on the pretreated $MgAl_2O_4$ (111) surface at 130 °C after the growth chamber was pumped to about 7.0×10^{-9} Torr. Then, the substrate temperature was increased to 260 °C for about 10 min. Finally, the same two-step growth of ZnO as sample A was used for growth of the films. No 30° rotation domains were found in sample B. It should be noted that different growth conditions were used for buffer and epilayer growths. A Zn beam flux of 1.2×10^{-6} Torr and a rf power of 240 W with an oxygen gas flux of 1.5 SCCM were adopted to form a zinc-rich condition for buffer, which is revealed to be significant for relaxation of misfit strain in ZnO film. Then, epilayer growth was performed under an oxygen-rich condition by using the same Zn flux and bigger rf power (400 W) and oxygen flux (2.0 SCCM), resulting in good electrical properties of ZnO film. Hall effect measurements using the van der Pauw method (Bio-Rad HL5200PC) showed that the background electron concentration of sample B is 6×10^{16} cm^{-3} and its electron mobility is 90 cm^2/V s at room temperature.

Figures 1(a) and 1(b) show the reflection high-energy electron diffraction (RHEED) patterns of sample A before and after ZnO buffer layer growth. Figure 1(a) is taken from the substrate surface right after the oxygen radical pretreatment. The sharp streaky RHEED patterns indicate a clean

[a)]Electronic mail: xldu@aphy.iphy.ac.cn
[b)]Electronic mail: qkxue@mail.tsinghua.edu.cn

 © 2007 American Institute of Physics
Downloaded 23 Feb 2007 to 159.226.36.135. Redistribution subject to AIP license or copyright, see http://apl.aip.org/apl/copyright.jsp

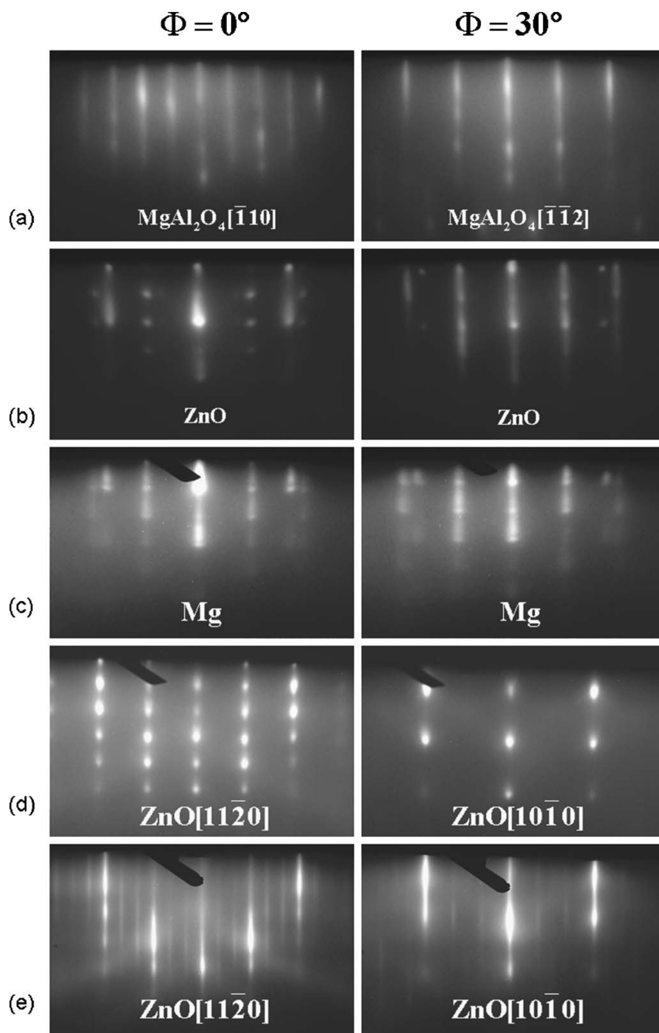

FIG. 1. RHEED patterns taken from (a) the clean $MgAl_2O_4$ (111) substrate, (b) during the ZnO buffer layer growth in sample A, (c) during the Mg deposition in sample B, (d) the annealed ZnO buffer layer in sample B, and (e) the ZnO epilayer in sample B, where the 3×3 surface reconstruction is clearly observed.

and flat surface after thermal cleaning and oxygen radical pretreatment. When ZnO buffer layer growth begins, a spotty RHEED pattern appears. Two sets of spots overlap together [Fig. 1(b)], which suggests that two kinds of domains coexist: one is the overlapped domain with an in-plane epitaxial relationship of $ZnO[11\bar{2}0]\|MgAl_2O_4[\bar{1}10]$ and the other has a 30° in-plane rotation along the [111] direction with respect to the overlapped domain.

On the other hand, 30° rotation domains are not observed in sample B. The same sharp streaky patterns as those from sample A [Fig. 1(a)] are observed after oxygen plasma pretreatment (not shown here). However, these patterns disappear immediately when a thin Mg layer is deposited on this O-terminated surface. It is clear that there are also two sets of RHEED patterns after deposition of the Mg layer [Fig. 1(c)], which suggests that there are also 30° rotation domains in the Mg layer. During the temperature ramping to 260 °C, the RHEED patterns from the Mg layer become dim and finally disappear. Almost the same RHEED patterns as those before Mg deposition appear again (not shown here). The result suggests that an ultrathin MgO wetting layer is formed, which was confirmed by the high-resolution transmission electron microscopy (HRTEM), as will be discussed later. When the ZnO buffer layer is deposited on the Mg-modified substrate surface, unlike sample A, only one set of spotty patterns is observed [Fig. 1(d)], and a single-domain ZnO with an in-plane epitaxial relationship of $ZnO[11\bar{2}0]\|MgAl_2O_4[\bar{1}10]$ is formed. The spotty patterns exist during the entire buffer layer growth [Fig. 1(d)] and become streaky gradually when the substrate temperature ramps to 650 °C. After growth at this temperature for 3 h, the sample surface appears very flat, as indicated by the sharp streaky 3×3 RHEED patterns in Fig. 1(e) and atomic force microscope (AFM) observation in Fig. 2. On an area of 1×1 μm^2, the root-mean-square roughness is only 0.389 nm. Atomically smooth steps, with a height of 2.6 Å corresponding to the bilayer step height along the c axis, are clearly resolved. The 3×3 is a typical surface reconstruction for the flat and uniform O-polar ZnO film,[3,10,11] the observations suggest that uniform O-polar ZnO film is formed, which is consistent with convergent beam electron diffraction experiment (not shown here).

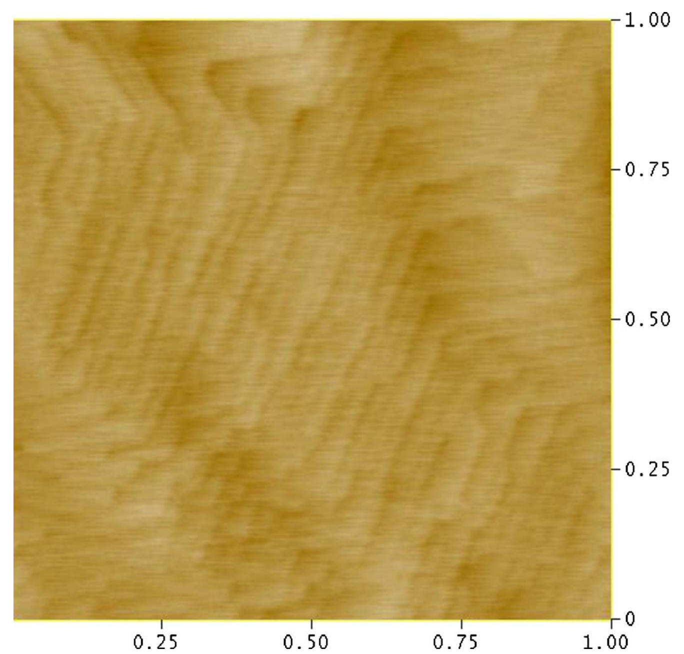

FIG. 2. (Color online) AFM image obtained from as-grown sample B. Image size is 1×1 μm^2.

To further determine the crystal quality, interface microstructure, and crystal orientation of the as-grown ZnO thin film, transmission electron microscopy observation was carried out. Figures 3(a) and 3(b) show the weak-beam dark-field cross-section TEM images along reflections (0002) and $(10\bar{1}0)$, which reflect the information on the screw and edge components of the dislocations, respectively. Three regions with different defect structures were found along the growth direction. Many defects exist in the region near the interface. It should be noted that three types of threading dislocations can be observed near the interface: edge, screw, and mixed dislocations. The density of dislocation amounts to 10^{11} cm^{-2}, as calculated according to $D=n/lh$, where n, l, and h are the number of the dislocations, the foil length, and the thickness in the cross-sectional specimen, respectively. In the middle region of the ZnO film, however, many dislocation loops were formed due to the strong interaction between screw components. Because of the annihilation of some screws and mixed dislocations by the loop information

Downloaded 23 Feb 2007 to 159.226.36.135. Redistribution subject to AIP license or copyright, see http://apl.aip.org/apl/copyright.jsp

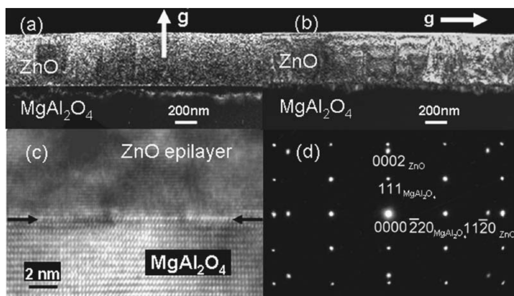

FIG. 3. Weak-beam dark-field cross-section TEM image along (a) $g=(0002)$ and (b) $g=(10\bar{1}0)$, (c)cross-sectional HRTEM image showing the $ZnO/MgO/MgAl_2O_4$ interface structure along ZnO $[10\bar{1}0]$, and (d) corresponding SADP of Sample B.

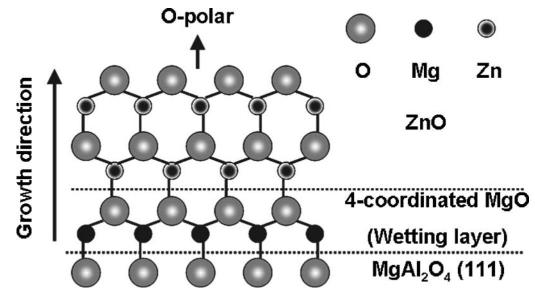

FIG. 4. Atomic model proposed for the interface structures between the MgO wetting layer and ZnO film in sample B.

in the middle region, the dislocation density in the upper region of the epilayer drops greatly to about 2.0×10^9 cm^{-2}. Figure 3(c) shows a cross-sectional high-resolution TEM image of the $ZnO/MgO/MgAl_2O_4$ interface region, taken along ZnO $[10\bar{1}0]$. It can be seen that the interface is atomically sharp without any amorphous layer or a layer with other structures. Hence, most of Mg atoms were reevaporated and about 1 ML of Mg was left via the formation of Mg–O bond on the substrate surface, which is consistent with the fact that the RHEED patterns almost recover after the substrate temperature ramping to 260 °C. Figure 3(d) shows the corresponding selected area diffraction pattern (SADP) near the interface region of sample B. The crystallographic orientation relationship is $ZnO[11\bar{2}0]\|MgAl_2O_4[\bar{1}10]$; no diffraction spots corresponding to the 30° rotation domain are found. By comparing the distance between the scattering and transmitting spots of ZnO and $MgAl_2O_4$, the misfit is estimated to be about 14.3%, very close to the theoretical value of 13.8% for the ideally aligned ZnO $(0001)/MgAl_2O_4$ (111) epitaxial system.

Obviously, the ultrathin MgO wetting layer plays a crucial role in the growth of single-domain O-polar ZnO film on $MgAl_2O_4$ (111) substrate. Such surface modification technique has been applied to ZnO epitaxy on several kinds of substrates.[7,8,12] In this study, we found that the mechanism also depends on the substrate. In the case of $MgAl_2O_4$ substrate, the O atoms and Mg atoms form a fcc-type structure with tetrahedral bonding, which influences the selection of the bond configuration of the MgO wetting layer. When the temperature increases to 260 °C, the Mg layer reevaporates due to the high vapor pressure of $\sim10^{-5}$ Torr; only one Mg layer bound to the topmost oxygen atoms on the substrate surface is left. The oxygen in the chamber will adsorp on this Mg layer, forming a uniform MgO wetting layer on the O-terminated $MgAl_2O_4$ (111) substrate. This MgO layer does not take its own structure, only overlaps on the oxygen sublattice of substrate, and inherits the tetrahedral bonding, i.e., each Mg atom forms a bond with the underlying O atom and three bonds with three oxygen atoms above. This tetrahedral-bonded MgO wetting layer acts as a uniform template for the epitaxy of O-polar ZnO film. Figure 4 shows a tentative atomic model of the interface between the MgO wetting layer and ZnO film based on our observations.

Direct deposition on the O-terminated $MgAl_2O_4$ (111) surface, on the hand, results in the formation of 30° rotation domain. We consider that it is mainly owing to the quasihexagonal structure of the oxygen sublattice in $MgAl_2O_4$ (111) plane due to the lattice distortion. There are two kinds of epitaxial orientations in the ZnO layers, which is similar to the growth of ZnO film directly on O-terminated sapphire (0001) substrate.[8] In sample B, however, the influence of distorted oxygen sublattice is eliminated completely by inserting a tetrahedral-bonded MgO wetting layer between the substrate and ZnO film, resulting in an O-polar ZnO film with a single domain. Furthermore, the strain in ZnO film caused by the big mismatch is relaxed by the two-step growth process, and a layer-by-layer growth is achieved finally.

In summary, by modifying the substrate surface using an ultrathin Mg layer, high-quality ZnO epitaxial films with atomically smooth surface have been achieved on the $MgAl_2O_4$ (111) substrate, and an atomic model is proposed to explain its effects on the 30° rotation domain elimination and O-polarity selection of ZnO films. Such quality films should be promising for preparing high performance quantum structures.

This work is financially supported by the National Science Foundation of China (under Grant Nos. 60476044, 60376004, and 50532090), Ministry of Science and Technology of China (under Grant No. 2002CB613502), and Chinese Academy of Sciences.

[1]D. C. Look, Mater. Sci. Eng., B **80**, 383 (2001).
[2]D. C. Look, D. C. Reynolds, C. W. Litton, R. L. Jones, D. B. Eason, and G. Cantwell, Appl. Phys. Lett. **81**, 1830 (2002).
[3]Y. F. Chen, H. J. Ko, S. K. Hong, and T. Yao, Appl. Phys. Lett. **76**, 559 (2000).
[4]J. W. Yang, Q. Chen, C. J. Sun, B. Lim, M. Zubair Anwar, M. Asif Khan, and H. Temkin, Appl. Phys. Lett. **69**, 369 (1996).
[5]C. M. Fang, S. C. Parker, and G. de With, J. Am. Ceram. Soc. **83**, 2082 (2000).
[6]Y. F. Chen, S.-K. Hong, H.-J. Ko, M. Nakajima, T. Yao, and Y. Segawa, Appl. Phys. Lett. **76**, 245 (2000).
[7]Z. Q. Zeng, Y. Wang, X. L. Du, Z. X. Mei, X. H. Kong, J. F. Jia, Q. K. Xue, and Z. Zhang, Sci. China, Ser. G **47**, 612 (2004).
[8]X. L. Du, M. Murakami, H. Iwaki, Y. Ishitani, and A. Yoshikawa, Jpn. J. Appl. Phys., Part 2 **41**, L1043 (2002).
[9]Z. X. Mei, X. L. Du, Y. Wang, M. J. Ying, Z. Q. Zeng, H. Zheng, J. F. Jia, Q. K. Xue, and Z. Zhang, Appl. Phys. Lett. **86**, 112111 (2005).
[10]Z. X. Mei, Y. Wang, X. L. Du, M. J. Ying, Z. Q. Zeng, H. Zheng, J. F. Jia, Q. K. Xue, and Z. Zhang, J. Appl. Phys. **96**, 7108 (2004).
[11]Y. F. Chen, H.-J. Ko, S.-K. Hong, T. Yao, and Y. Segawa, J. Cryst. Growth **214/215**, 87 (2000).
[12]M. J. Ying, X. L. Du, Y. Z. Liu, Z. T. Zhou, Z. Q. Zeng, Z. X. Mei, J. F. Jia, H. Chen, Q. K. Xue, and Z. Zhang, Appl. Phys. Lett. **87**, 202107 (2005).

Downloaded 23 Feb 2007 to 159.226.36.135. Redistribution subject to AIP license or copyright, see http://apl.aip.org/apl/copyright.jsp